

The Cyclopropylmethyl–3-Butenyl Rearrangement on Mo(110): A Radical Clock on a Surface?[†]

Beate Flemmig,[‡] Ilona Kretzschmar,[§] Cynthia M. Friend,^{||} and Roald Hoffmann^{*,‡,⊥}

Department of Chemistry and Chemical Biology, Cornell University, Baker Laboratory, Ithaca, New York, 14853-1301, Department of Electrical Engineering, Yale University, New Haven, Connecticut, 06511, and Department of Chemistry, Harvard University, Cambridge, Massachusetts, 02138

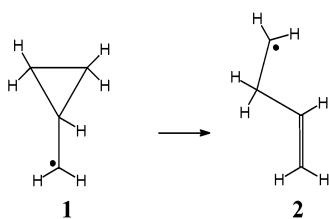
Received: October 3, 2003; In Final Form: January 17, 2004

The mechanism for the transformation of adsorbed cyclopropylmethoxy into its ring-opened form, 3-butenyloxy, on the Mo(110) surface is explored theoretically. An alternative emerges to the radical clock mechanism that involves the cleavage of the C–O bond in the adsorbate as the critical reaction step. The alternative pathway involves the cleavage of a C–C bond in the three-membered ring leading to a diradical, which could transform via a 1,2-H shift to the same reaction product. Density functional theory (DFT) calculations for relevant reaction intermediates in molecular model systems show an energetic preference for the C–C cleavage in the initial step. The barrier of the subsequent 1,2-H shift of the singlet diradical is slightly lower than the barrier for the radical clock rearrangement, rendering the diradical pathway a possible alternative. Adsorbate structures for the reactant and the product were obtained by DFT slab calculations. We carry out a MO analysis of the bonding in the adsorbate, comparing also C–C and C–O bonding.

Introduction

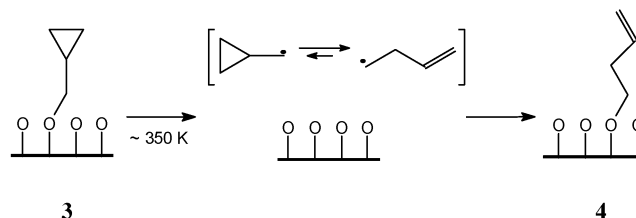
Radical clocks are an established tool in organic chemistry for probing the existence of radical reaction intermediates and estimating their lifetimes.¹ The clocks are themselves radicals that, once they are generated as a free species, undergo a characteristic rearrangement reaction on a well-known time scale. Thus, a radical clock system as a substituent at a certain atom serves as an indicator for the formation of a radical with a certain lifetime at this specific site in the molecule.²

A collection of calibrated alkyl radical clocks was provided by Ingold.³ The system with the shortest lifetime ($\sim 10^{-8}$ s) from the so-called primary alkyl horlogerie, is the cyclopropylmethyl radical **1**. It rearranges very rapidly by breaking the three-membered ring to form the 3-butenyl radical **2**.



Recently, this same type of rearrangement has been observed in the vicinity of an oxygen-covered molybdenum surface.⁴ More precisely speaking, FT-IR measurements obtained at different temperatures indicated the formation of the adsorbed 3-butenyl species **4** above 350 K from adsorbed cyclopropylmethyl **3**, both attached to surface oxygen. This was possible because the three-membered ring and the double bond are very

clearly distinguishable by their characteristic vibrations: 1394 and 1433 cm^{-1} for the ring and 1646 cm^{-1} for the double bond. The conclusion drawn is that the C–O bond in the adsorbate breaks at the elevated temperatures to yield the free radical clock cyclopropylmethyl, which lives just long enough to undergo the rearrangement before it gets trapped again at the surface.



It seems then possible to use radical clocks as mechanistic and kinetic probes for surface reactions. Related radical clock systems with slightly different lifetimes in the gas phase have been studied on this surface as well and show the analogous rearrangement.⁵ This development is particularly interesting, as radicals are invoked as key intermediates for a number of catalytically relevant surface reactions,⁶ while information on the mechanisms of these reactions is still rare. It has been shown recently that the lifetime of the radical clock systems is affected by the influence of metal ions.⁷ Thus, it is also likely that the surface influences the lifetime. New radical clocks with even shorter lifetimes than the lifetime of the cyclopropylmethyl radical have been proposed in a recent computational study. These are the isoelectronic cyclopropoxy radical and cyclopropylaminium radical cation.⁸ Before we address these issues, we need to be sure that the surface reaction mechanism indeed involves the radical clock.

Thus, it is crucial to learn more about the reaction of the cyclic alkoxide **3** to the ring-opened alkoxide **4**, both proven spectroscopically to exist on the surface. The formation of the cyclic alkoxide on the surface was observed for different

[†] Part of the special issue "Fritz Schaefer Festschrift".

^{*} Author to whom correspondence may be addressed. E-mail: rh34@cornell.edu.

[‡] Cornell University.

[§] Yale University.

^{||} Harvard University.

[⊥] Dedicated to our friend Fritz Schaefer.

precursor molecules, cyclopropylmethylbromide⁹ and cyclopropylmethanol,⁵ which were dosed in small concentrations onto the surface. In the first case, the alkyl moiety is transferred, obviously without rearrangement, onto a surface oxygen. This process may be viewed as a S_N2 reaction with bromide as a leaving group. In the second case, the O–H bond of the alcohol dissociates at the oxygen-covered surface, leading to the formation of surface OH groups, which could be detected spectroscopically by their characteristic band at 3560 cm⁻¹. The alkoxide binds through its oxygen atom to a free surface Mo atom. Thus, different routes for different precursor systems lead to the observed cyclic alkoxide on the surface, which rearranges subsequently to the ring-opened form.

The radical clock mechanism for the rearrangement hinges on two suppositions: first, that the C–O bond breaks to form the cyclopropylmethyl radical and, second, that the radical stays long enough near the surface, once it is formed. Weak interactions that would hold the free radical in the vicinity of the surface are difficult to characterize. But, the other prerequisite for this reaction pathway, the cleavage of the C–O bond upon thermal excitation of the adsorbate, can be addressed theoretically. In this and subsequent papers, we study the cyclopropylmethyl radical clock reaction and related reactions on surfaces.

Computational Details

For the surface slab calculations, the plane-wave density functional theory (DFT) code fhi98md¹⁰ was used. It employs pseudopotentials representing the core and inner electrons of the atoms. The Troullier–Martins type of pseudopotential¹¹ was chosen for this study and generated with the fhi98pp code.¹² The transferability of the pseudopotentials was tested and the absence of unphysical ghost states was verified using Gonze’s analysis.¹³ With a cutoff energy of 60 Ry for the plane-wave expansion, the total energy per atom in the adsorbate slab converged within 0.01 eV/atom. The sampling of the k space employed a 4 × 4 × 1 Monkhorst–Pack mesh¹⁴ (4 × 4 × 4 for bulk calculations).

As a first test calculation, the bulk lattice constant of the bcc Mo lattice was optimized, yielding 3.096 Å using the LDA functional¹⁵ and 3.155 Å for the Becke–Perdew GGA functional.¹⁶ The accepted experimental value¹⁷ is 3.147 Å. In accordance with general experience, LDA underestimates the lattice parameter whereas GGA overestimates it slightly. The difference of 0.25% between the GGA result and the experimental value is acceptable.

In another test calculation, the surface relaxation was calculated using slabs with three, four, and five atomic layers with a vacuum spacing of 15 Å between the slabs. The first atomic layer was allowed to relax, and the others were kept fixed at the optimized bulk positions. Atomic positions were allowed to relax until the residual forces were below 0.01 eV/Å. The relaxation of this stable surface has a minor structural effect, the first interlayer spacing d_{12} decreases slightly. Experimentally¹⁸ this contraction relative to the bulk distance has been found to be $\Delta d_{12} = -1.6 \pm 2\%$, corresponding to an absolute value for the contraction of only 0.03–0.07 Å. The calculation with the three-layer slab resulted in $\Delta d_{12} = -4.7\%$, already a reasonable value. Four- and five-layer slab calculations yielded smaller contractions of around -1%.

For the molecular DFT calculations, we used the B3LYP¹⁹ hybrid functional as implemented in the Gaussian 98 package.²⁰ The unrestricted formalism was applied for open-shell species. The LanL2DZ basis set option was used applying a Dunning–Huzinaga-type full double- ζ basis²¹ set for C, O, and H and a

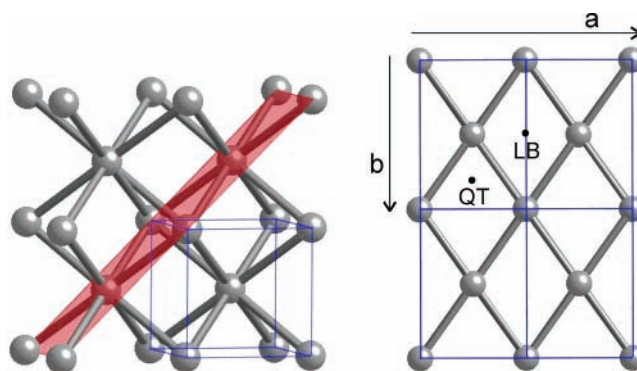


Figure 1. (110) plane in the bcc lattice and in a top view of the surface. a and b indicate the lattice vectors of the chosen surface unit cell; labeled dots indicate quasi-3-fold and long-bridge adsorption site

TABLE 1: Extended Hückel Parameters

atom	orbital	H_{ii} (eV)	ζ_1	c_1	ζ_2	c_2	ref
Mo	5S	-8.34	1.96				24
	5P	-5.24	1.90				
	4D	-10.5	4.54	0.5899	1.9	0.5899	
C	2S	-21.4	1.625				25
	2P	-11.4	1.625				
O	2S	-32.3	2.275				25
	2P	-14.8	2.275				
H	1S	-13.6	1.3				25

Los Alamos effective core potential²² along with a double- ζ basis set for Mo. All structures were fully optimized, except for a few special cases where this is explicitly stated. Frequency analyses were carried out for all fully optimized structures to characterize the obtained minima and transition states (TSs). Reported relative energies based on fully optimized structures are zero-point-energy corrected and thermally corrected (298 K).

Extended Hückel calculations (eH) based on the optimized structures for the molecular systems as well as for the infinite slabs were performed with the YAEHMOP package,²³ which allows also eH calculations with periodic boundary conditions. The standard atomic Hückel parameters for Mo, C, O, and H were used and are listed in Table 1. Visualization of molecular orbitals was carried out with the CACAO program.²⁶ To visualize MOs of extended structures, sufficiently large finite systems were generated that could be treated with CACAO.

Results and Discussion

I. Surface Slab Calculations. To determine reliable adsorbate geometries, we used DFT slab calculations. The fhi98md code allows geometry optimization for extended systems. Test calculations for the surface relaxation showed that a three-layer slab is sufficient for our purposes. The surface unit cell has to be chosen to be sufficiently large to avoid severe steric problems between the adsorbed organic molecules. We chose a surface unit cell consisting of two adjacent centered rectangles in the a direction of the Mo (110) plane, as indicated by the lattice vectors a and b in Figure 1. Important adsorption sites on this surface are the quasi-3-fold (QT) and the long-bridge position (LB).²⁷

An oxygen overlayer with a coverage of $\theta = 2/3$ (as used in the experiments and analyzed with LEED)⁹ requires a surface unit cell that consists of three adjacent centered rectangles in the b direction. A calculation of the adsorbed molecule including the real oxygen coverage would therefore necessitate a large surface unit cell consisting of six centered rectangles (two in the a and three in the b direction). This is currently not possible

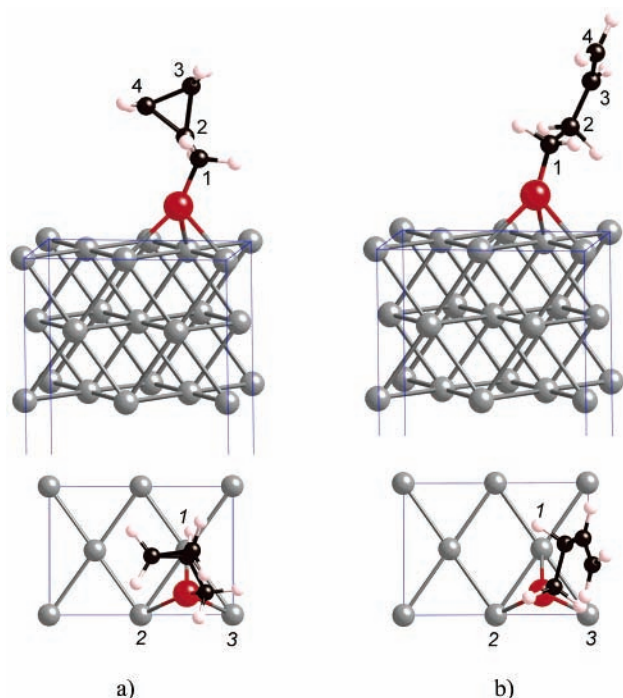
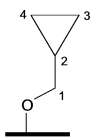
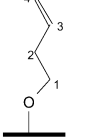
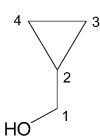


Figure 2. Optimized structures of (a) cyclopropylmethoxide and (b) 3-butenyloxide on Mo (110). The atom numbering for the adsorbed molecules carries no mechanistic implication. Italic atom numbers refer to Mo atoms.

TABLE 2: Selected Bond Lengths in the Optimized Structures of Cyclopropylmethoxide and 3-Butenyloxide on Mo (110) in Comparison with Isolated Cyclopropylmethanol

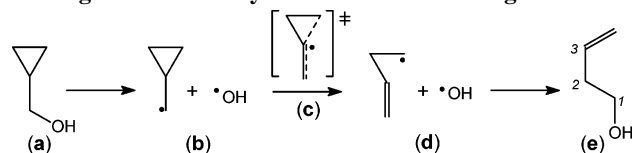
$r/\text{\AA}$			
Mo1–O	2.153	2.174	
Mo2–O	2.439	2.364	
Mo3–O	2.416	2.347	
O–C1	1.613	1.580	1.519
C1–C2	1.497	1.545	1.525
C2–C3	1.551	1.502	1.542
C3–C4	1.536	1.362	1.537
C2–C4	1.581		1.548

for us to do. With the surface unit cell shown above, which includes 4 Mo atoms, we could model coverages of $\theta = 1/2$ and $\theta = 1/4$ (i.e., include two or one O atoms per unit cell).

For the calculations presented here, we chose to include the alkoxide species in the unit cell, which corresponds formally to an oxygen coverage of $\theta = 1/4$. (We are aware of the fact that the probability of trapping again the emerging radical after its rearrangement at the surface might well be dependent on the number of available surface oxygen atoms. In fact, the amount of 3-butenyl oxide yielded by selective reaction increases with oxygen coverage in the experiments.) The adsorbate geometries, however, are not likely to be influenced much by additional adsorbed oxygen.

Geometry optimizations of cyclopropylmethoxide and of 3-butenyloxide on the Mo (110) surface resulted in the adsorbate structures shown in Figure 2 and Table 2. For these calculations, the Mo atoms of the slab were fixed to the ideal bulk positions. (Calculations of the slab with an oxygen overlayer and the first Mo layer allowed to relax showed that this is reasonable and that the position of these atoms is not affected much by an

SCHEME 1. Radical Clock Reaction Mechanism Starting with a Homolytic C–O Bond Cleavage



adsorbate.)²⁸ In the optimized structure, the oxygen atom of the alkoxides adopts a quasi-3-fold adsorption site with one short Mo–O bond (~ 2.2 Å) and two longer Mo–O bonds (~ 2.4 Å).

In accordance with the experimental observation, we obtain a lower total energy for the reaction product, the adsorbed ring-opened alkoxide. The energy difference between the two structures shown is 31.0 kJ/mol. Other conformers of the molecules, which result from rotations around the C–O bond and the C–C single bonds, are expected to cause at most an energetic effect of 2 kJ/mol, based on molecular calculations. An optimization of the isolated cyclopropylmethanol molecule in the gas phase with the same method (using a large unit cell with a lattice constant of 25 Å) shows the structural effects of the chemisorption. Mainly, the C–O bond of the molecule is noticeably elongated in the adsorbate by 9 pm, which is in the range of what was found before in adsorbates of organic molecules.²⁹ Closer inspection of Table 2 shows that the C–O bond for the cyclic species is slightly longer than that of the linear species (1.613 vs 1.580 Å).

It is not practical to pursue alternative reaction mechanisms and calculate all possible reaction intermediates at this high level of theory. Moreover, the treatment of open-shell species with broken bonds, required here, is inherently not easy, as the definition of the spin state in periodic calculations is not well determined. At the same time, there is a lot of experience and lore on adequate procedures for treating bond breaking and diradicals in discrete molecular systems. We therefore turn to smaller model systems to limit and yet more definitely define the search for the mechanism of the surface reactions.

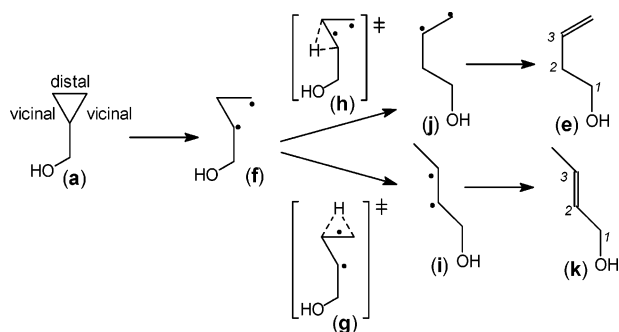
II. The Intrinsic Reactivity of the Molecule. How would the molecule in the gas phase, were it not bound to the surface, transform from the cyclic to the ring-opened form? Several reaction pathways from cyclopropylmethanol to 3-butenol come to mind. In principle, there are two main routes; one starts with the cleavage of the C–O bond (which can happen homo- or heterolytically), and the other one proceeds via an initial cleavage of a C–C bond in the cyclopropyl ring.

Homolytic cleavage of the C–O bond would lead to the cyclopropylmethyl radical and thus to the radical clock reaction, as shown in Scheme 1. The corresponding carbocation resulting from a putative heterolytic cleavage can also undergo this rearrangement very easily.³⁰

The other main alternative, C–C cleavage (Scheme 2), would not lead to a fragmentation of the system into two parts. It would instead yield a diradical (**f**), which we, in a first approximation, assumed to be a triplet diradical. The possibility of a singlet diradical was investigated³¹ and proved to be relevant too.

With respect to singlet and triplet diradical (**f**), the important singly occupied MOs are the same as for the well-studied trimethylene diradical³² and are shown in **5** and **6**.



SCHEME 2. Diradical Reaction Mechanism Starting with the Cleavage of a Vicinal C–C Bond^a


^a The species **j** and **i** are only relevant in the triplet case.

In the triplet state, these two MOs are occupied by electrons with parallel spin, whereas in the singlet case, they are occupied by electrons with opposing spin. For the parent trimethylene system, the minimum for the singlet diradical is very shallow. Therefore, some of the calculations report a singlet diradical³³ and some do not.³⁴ The existence of the singlet trimethylene diradical is now generally agreed on;³⁵ indeed, a femtosecond lifetime for this species has been determined.³⁶

There are two variations for the C–C cleavage: one is the cleavage of the vicinal bond, as shown in Scheme 2. The other possibility is the cleavage of the distal C–C bond, leading to a diradical with two primary carbon radicals. The diradicals formed from the cleavage of a C–C bond stabilize themselves by a 1,2-H shift. If a vicinal C–C bond is broken, an H atom from the unaffected carbon of the cyclopropyl ring may move to either the primary or the secondary radical carbon next to it, leading to final products 2-butenol and 3-butenol, respectively. If the diradical route were followed, both isomers are likely to be formed. The butenyl species with the doubly substituted C=C bond, 2-butenol, is expected to be found in higher concentrations because the 1,2-H shift toward the primary carbon atom is likely to be slightly preferred.

By means of DFT calculations, we were able to follow these four reaction paths, homolytic and heterolytic C–O bond cleavage and distal and vicinal C–C bond cleavage. We compare the relative energies (with respect to cyclopropylmethanol) of intermediates and TSs along these pathways in Figure 3. Note several things about Figure 3, of necessity complex, because it tries to represent several pathways. The left most sequence is the radical clock. The right most is the singlet diradical route. The central sequence follows the triplet diradical route showing only triplets except the reactant and the products.

Two alternatives could be excluded right away (not shown in Figure 3) by inspection of the first intermediates. One is the heterolytic C–O bond cleavage, which requires, not unexpectedly, a very high energy ($E_{\text{rel}} = +950$ kJ/mol), in the gas-phase reaction. The actual energy required for a heterolytic cleavage might be lower. In the surface reaction, the surface could act as a kind of solvent. The surface could stabilize both components of a heterolytic cleavage, the anionic part by accepting its electrons into empty surface bulk states and the cationic part by image charge stabilization (effectively screening the charge). The details of this stabilization remain to be worked out. In future work, we will come back to the solvent-like properties of surfaces. The other possibility that appears as relatively unlikely is the homolytic cleavage of the distal C–C bond. The resulting diradical with two primary radicals is slightly higher

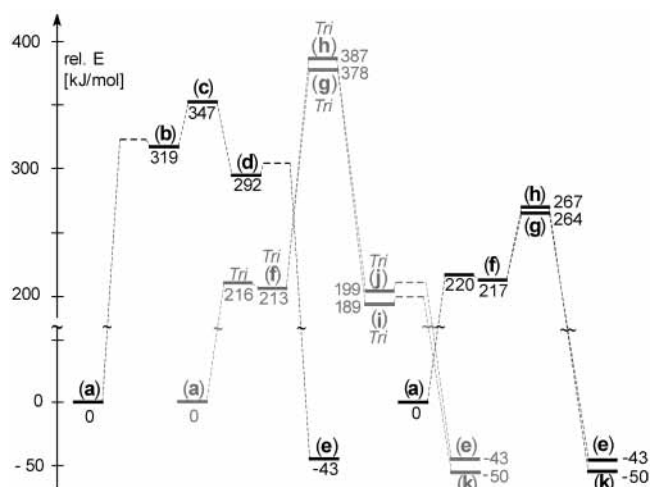


Figure 3. Energy profiles for the two reaction paths involving the radical clock (**b**) or the diradical (**f**) in the triplet and singlet state. Triplet species are marked with *Tri*. Dashed horizontal lines indicate estimated energies of TSs for dissociation and radical recombination that were not calculated. The structure labels (**a**)–(**k**) refer to Schemes 1 and 2.

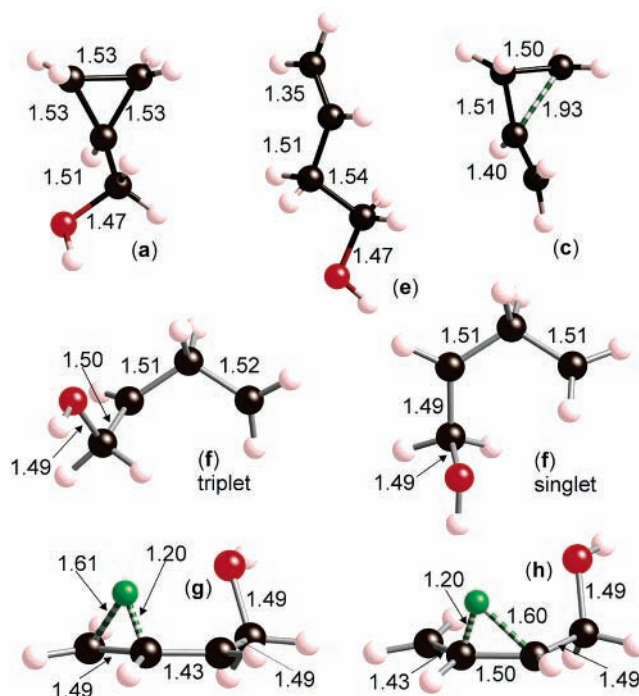


Figure 4. Calculated structures of selected species along the reaction paths: (**a**) cyclopropylmethanol; (**e**) 3-butenol; (**c**) TS of the radical clock rearrangement, a doublet; (**f**) diradical after breakage of vicinal C–C bond in singlet and triplet state (*Tri*); (**g**) TS of the 1,2-H shift toward the primary carbon radical in the singlet state; (**h**) TS of the 1,2-H shift toward the secondary carbon radical in the singlet state. Striped bars indicate breaking and forming bonds in the TS.

in energy (by 6 kJ/mol) than the diradical emerging from the cleavage of the vicinal C–C bond.

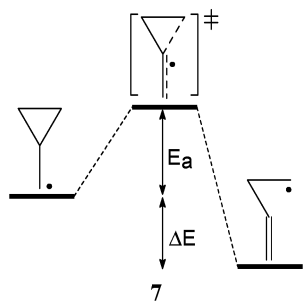
Thus, the radical clock mechanism and the diradical mechanism are the two alternatives that have to be considered. Optimized geometries of selected species along the two alternative pathways are shown in Figure 4. The calculated atomic spin densities for the open-shell species are shown in the Appendix. These show spin distributions that are as expected for the various triplet, doublet, and singlet states. As can be seen from the relative energies in Figure 3, the C–C bond breakage is clearly preferred over the breakage of the C–O bond

in the initial step. (We presume that these highly endothermic first steps are not activated much over and above their thermodynamic energy difference.) In fact, this is not surprising, as the lability of the cyclopropyl ring toward C–C cleavage is well known for strained systems^{37,38} and is used for instance in the activation of aliphatic molecules.^{39,40}

The singlet, as well as the triplet, diradical resulting from the C–C cleavage was considered. The triplet and the singlet diradicals proved to be very similar in energy. The following reaction step on the diradical route, the 1,2-H shift, however, is different for singlet and triplet state. The TS for the H-shift of the singlet is considerably lower than the one for the triplet. This is understandable, because in the singlet TS the C=C double bond can already be partially formed. This is indicated by the coplanar arrangement of the terminal methylene group. In the triplet TS, this CH₂ group is oriented perpendicular to the σ frame of the molecule (see (h) in Figure 4), consistent with an ethylene triplet geometry.

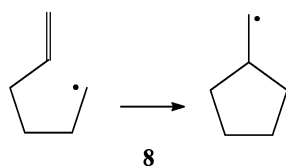
The 1,2-H shift is the rate-determining step (the step with the highest-lying TS)⁴¹ on the singlet diradical route. We obtain a TS for the H-shift of the singlet diradical that is lower than the TS of the radical clock rearrangement.

We can compare the energetics of our singlet diradical route with the well-studied isomerization of cyclopropane to propene via singlet trimethylene.^{35,42} The activation barrier for the C–C cleavage was found to be around 230 kJ/mol (55 kcal/mol). The subsequent barrier for the 1,2-H shift was estimated to be in the order of 25 kJ/mol (6 kcal/mol). Our values for the substituted system are in the same range (compare with Figure 3).



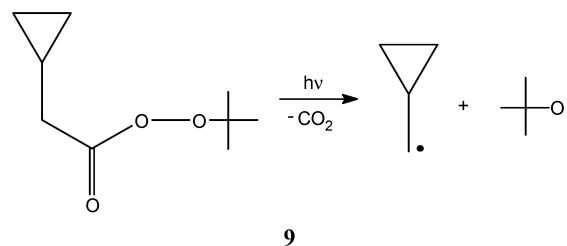
The calculations also yield thermodynamic and kinetic information for the gas-phase radical clock system **7** (which is available from experiment and theory on a range of different levels)⁴³ and, thus, provide us with another chance to evaluate our calculations. We obtain an activation barrier E_a for the radical clock of 27.5 kJ/mol and a ΔE value of -26.8 kJ/mol. Among the reported experimental values are 24.9 kJ/mol⁴⁴ for E_a and -21.0 kJ/mol⁴⁵ for ΔE . The current best calculations available using the CBS-RAD method⁴³ give 31.2 kJ/mol for E_a and -10.8 kJ/mol for ΔE .

In general, the strain in the three-membered ring is obviously the driving force for the reaction. The distinction between the two alternative mechanisms is merely whether the ring breaks first to yield a diradical or the C–O bond breaks first to yield two radicals, of which one would then open the ring. The ring strain energy of cyclopropane is 116 kJ/mol.⁴⁶ Incidentally, the



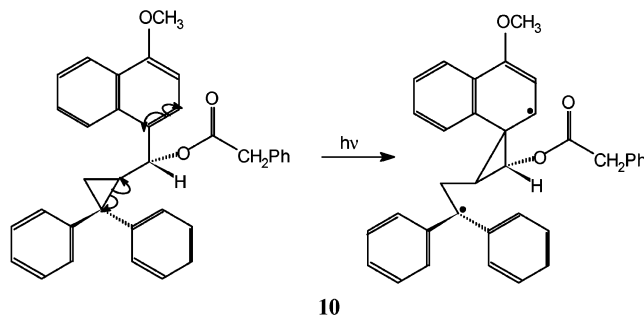
radical clock for the five-membered ring homologue **8**, also part of the primary alkyl horlogerie³, reacts via ring closure. The experimentally determined ring strain for cyclopentane is 21 kJ/mol⁴⁶ and significantly lower than that for cyclopropane.

In the surface context, the question arises how the cyclopropylmethyl radical clock can be formed without the complication of the ring cleavage. In organic applications^{1,2} as well as in the calibration^{3,44} of the system, the reaction conditions were somewhat different. In studies of organic reactions, the radical clock is formed from a nonradical precursor, in the simplest case by H abstraction.¹ In the calibration of the radical clock, a photolabile precursor molecule⁴⁴ was used, as shown in **9**. The cyclopropylmethyl *tert*-butyl peracetate undoubtedly decays into radicals and CO₂ upon exposure to light. Other precursors are, for example, azoalkanes.²

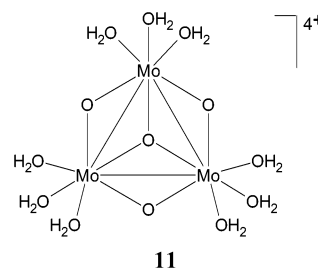


In one example,⁴⁷ **10**, the tentative precursor system, an ester that was expected to break the C–O bond upon excitation, reacts via cyclopropyl bond cleavage. In this specific case, it was concluded that this is caused by the steric orientation of the chromophore, the 4-methoxy-1-naphthyl substituent, which induces the formation of a diradical rather than excitation of the C–O bond.

On the basis of our calculations, we are not prepared to rule out either of the two alternatives on the surface. An oxygen atom on a surface might bind to the cyclopropylmethyl moiety with a much different strength than the oxygen in the isolated cyclopropylmethanol molecule. This would yield a C–O bond that is more likely to break than a C–C bond of the ring, thus favoring the radical clock pathway even more – also in the initial step.

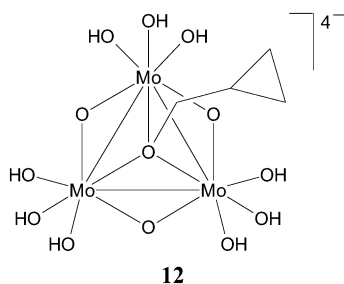


III. A Molecular Model System. To model the chemical environment of the adsorbed molecule somewhat realistically



yet remain with a molecular system, the cluster approach is the method of choice. Though widely and successfully applied for ionic or covalent substrates,²⁹ for metals the usual saturation or passivation strategies (point charges or hydrogen atoms) are not chemically intuitive. If metal clusters are used, they are often not saturated at all⁴⁷ or treated with special embedding techniques.⁴⁸

In this specific case, we chose to base our cluster model on a well-known molybdenum compound, the trinuclear cluster $[\text{Mo}_3\text{O}_4(\text{H}_2\text{O})_9]^{4+}$, **11**, which is abundant in aqueous solutions of Mo^{IV} . It is also found in crystal structures with some variations on the water ligands (e.g., exchange by oxalato ligands).^{50,51} The cluster is related to a large family of triangular Mo clusters with single Mo–Mo bonds.⁵² Calculations of the oxygen overlayer on Mo showed that the oxygen adopts quasi-3-fold and long-bridging sites, which are clearly geometrically similar to this compound.²⁸ Also, the surface Mo atoms are slightly oxidized, which justifies the use of a Mo^{IV} cluster.



For the actual cluster model, the nine water ligands were exchanged for nine OH^- ligands (to reduce the number of orientational degrees of freedom), which leads us to a species $[\text{Mo}_3\text{O}_4(\text{OH})_9]^{5-}$. We want to attach the organic molecule in the 3-fold position (the oxygen is already there). Thus, we bring in the alkyl part as a cation, formally, and calculate the system $[\text{Mo}_3\text{O}_4\text{C}_4\text{H}_7(\text{OH})_9]^{4-}$. If we were to add the alkyl as a radical, we would end up with an open-shell system for the model reactant. Compound **12** shows the reactant, the cyclic alkoxide, in the cluster model. By use of this model, we follow again the two main alternative mechanisms, diradical mechanism and radical clock path. Figure 5 shows optimized structures for species along these routes. Relative energies and C=C stretching frequencies are shown in Table 3 along with the data for the isolated molecules for comparison.

In general, the cluster calculations follow the trend of the intrinsic (i.e., gas-phase calculated) reactivity of the molecule. However, the differences between the two pathways are significantly diminished if one takes into account some aspects of the surface. The energy of the 1,3 diradical species formed from an initial C–C cleavage is by some kJ/mol lower than the energy of the two fragments, cyclopropylmethyl and $[\text{Mo}_3\text{O}_4(\text{OH})_9]^{4-}$, resulting from a C–O bond cleavage. Note that the difference between the C–O cleavage and C–C cleavage in the cluster model is very small. This is mainly due the distribution of the radical character of $\cdot\text{OR}$ over the Mo atoms of the cluster. The barrier for the 1,2-H shift on the diradical pathway is again slightly lower than the one for the rearrangement of the radical clock radical, if the singlet state of the diradical is considered. However, the energy difference between the TS of the radical clock rearrangement and the 1,2-H shift is, in our cluster model, so small (compare in Table 3 the relative energies for the 1,2-H-shift TS of 222 kJ/mol and the TS of the radical clock rearrangement of 227 kJ/mol) that we cannot conclude from this which mechanism would be preferred.

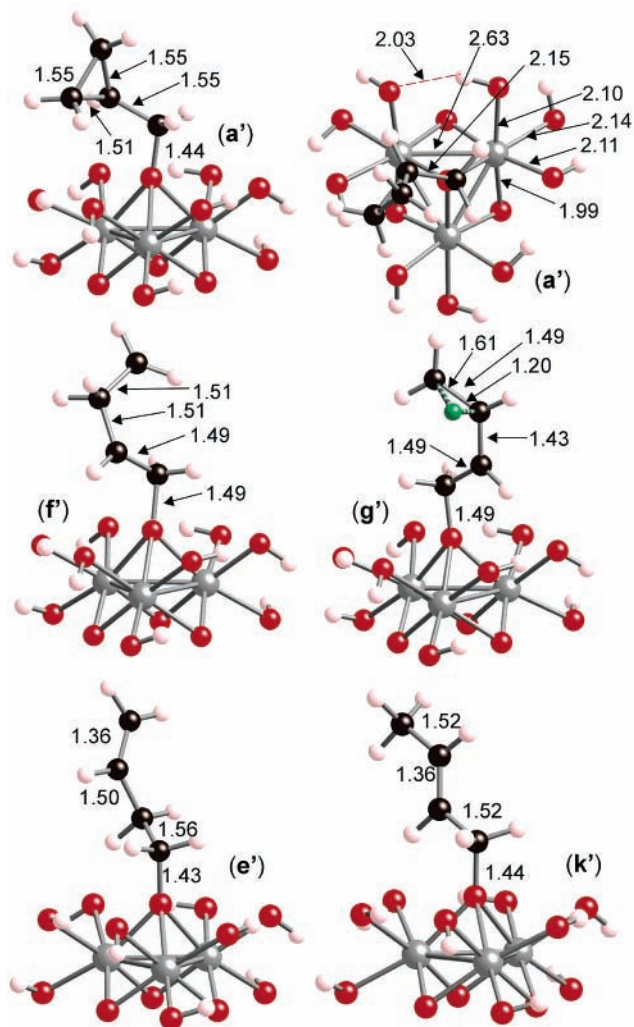
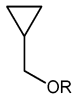

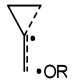

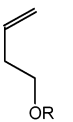
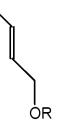
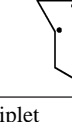

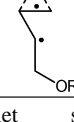


Figure 5. Optimized geometries of selected species $[\text{Mo}_3\text{O}_4\text{C}_4\text{H}_7(\text{OH})_9]^{4-}$ along the two reaction paths. (a') Cyclopropylmethoxide on $[\text{Mo}_3\text{O}_4(\text{OH})_9]^{4-}$, distances in molecule indicated at left (side view) and in cluster at right (top view); (f') 1,3 diradical in the singlet state; (g') TS for the 1,2-H shift toward the primary carbon radical in the singlet state; (e') 3-butenoxide; (k') 2-butenoxide. Singlet diradical species (f' and g') were calculated at the optimized geometry of the corresponding isolated molecules.

We point out that the energy for the radical $[\text{Mo}_3\text{O}_4(\text{OH})_9]^{4-}$ (which is a Jahn–Teller system with three electrons in two degenerate MOs of e symmetry) is based on a single point calculation at the geometry of the cluster part of the systems containing the molecule $[\text{Mo}_3\text{O}_4\text{C}_4\text{H}_7(\text{OH})_9]^{4-}$. The geometry of the $\text{Mo}_3\text{O}_4(\text{OH})_9$ unit of these systems does not differ significantly for the various alkyl groups attached (cyclopropylmethyl, butenyl, or diradical). Bond distances and angles of the same type are almost equal, consistent with the C_3 pseudosymmetry of the cluster part of the systems. If we allow deformations, the $\text{Mo}_3\text{O}_4(\text{OH})_9$ radical species without the alkyl bound undergoes a strong Jahn–Teller distortion, which makes the three Mo–Mo bonds unequal (calculated Mo–Mo bond lengths 3.28, 2.83, and 2.69 Å). If our energetic comparison were based on the energy of the optimized $[\text{Mo}_3\text{O}_4(\text{OH})_9]^{4-}$ unit, the initial C–O cleavage would be preferred because of the stabilization of the distorted Mo cluster. This distortion, however, is a result of the finite size of our cluster model, and we do not consider it relevant for modeling the surface reaction.

An interesting effect in the cluster model, relevant to the surface chemistry, is the depletion of spin density at the radical

TABLE 3: Calculated Relative Energies in kJ/mol and C=C Stretching Frequencies in cm^{-1} of Cluster Species $[\text{Mo}_3\text{O}_4\text{C}_4\text{H}_7(\text{OH})_9]^{4-}$ and Molecular Species $\text{C}_4\text{H}_7\text{OH}$ along Two Alternative Reaction Paths (TSs Indicated by Dashed Bonds)

										
							triplet	singlet	triplet	singlet
R: $\text{Mo}_3\text{O}_3(\text{OH})_9^a$	0	199	227	173	-61	-52	188	196 ^c	355	222 ^c
R: H^b	0	319	347	292	-43	-50	213	220	378	264
	Frequency									
R: $\text{Mo}_3\text{O}_3(\text{OH})_9^a$				1696	1650	1689				
R: H^b				1696	1702 ^d	1743 ^c				

^a The spin state of radical fragments is doublet, of diradicals is triplet and singlet as indicated, and of closed-shell systems is singlet. ^b $\langle S^2 \rangle$ values after spin annihilation for all open-shell species differ by not more than 3×10^{-3} from expected values of 0.75 for doublets and 2.0 for triplets. ^c Single-point calculation for singlet diradical cluster species at optimized geometry of the isolated molecules. ^d Experimental value for gas-phase species (NIST database): 1641 cm^{-1} . ^e Experimental value for gas-phase species (NIST database): 1675 cm^{-1} .

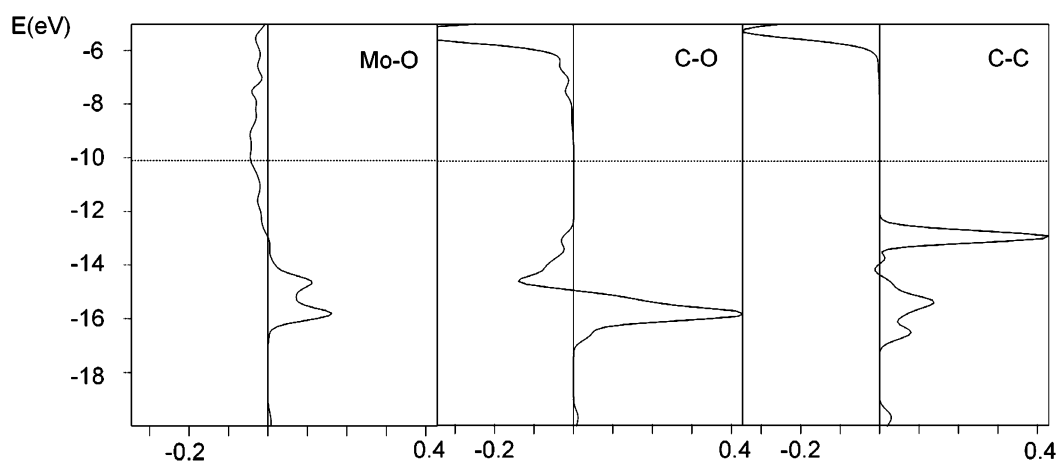


Figure 6. COOPs for the Mo–O bond, the C–O bond, and one vicinal C–C bond of the three-membered ring in the adsorbate of cyclopropylmethoxide on a 3-layer Mo(110) slab. Computed total overlap populations Mo–O 0.26, C–O 0.41, and C–C 0.62. The dotted line is the Fermi energy.

carbon atoms in the diradical species relative to the isolated molecules (see calculated spin densities in the Appendix). Obviously, the metal atoms of the substrate can accommodate, at least partially, unpaired electrons from the adsorbed species. This could be the reason, overall, why the energetic barriers that have to be overcome for the reaction are lower in the cluster model (and presumably also on the surface) than in the isolated gas-phase molecules.

The frequency analyses for the molecular species showed, in agreement with the experimental data, a C=C stretching normal mode around 1700 cm^{-1} that does not involve other motions in the molecules. A similarly distinct C–O stretching mode is not found; the C–O stretching motion is strongly coupled to other motions in the system.

IV. MO Analysis of the Bonding in the Adsorbate.

Analysis of bonding in surface reactions is often easier if one looks at a simpler one-electron calculation. This led us to try periodic eH calculations, performed using the optimized adsorbate slab geometries from the DFT slab calculations. By means of the crystal orbital overlap population (COOP), we can obtain information on contributions to bonding at various energies.

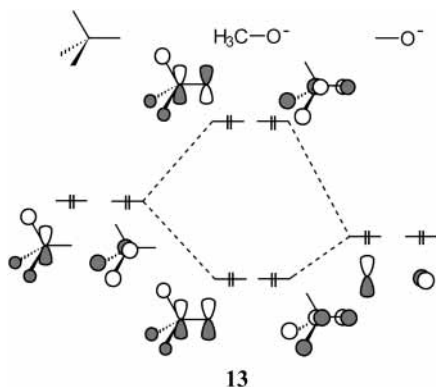
Figure 6 shows this analysis for the Mo–O, C–O, and C–C bonds in the adsorbed cyclic alkoxide, the reactant under consideration. As expected, all three interactions are overall bonding in character, which is obvious from the (on balance) positive COOP curves up to the Fermi level. Further, it can be seen that the dominant regions of Mo–O and C–O bonding

lie effectively below the C–C bond in energy. In fact, the C–C bonding levels are the highest occupied orbitals primarily localized on the adsorbate. The DOS (density of states) and band structure, not shown here, do have higher-lying crystal orbitals up to the Fermi level. But these are merely related to the substrate and involve Mo atoms other than the three interacting with the molecule.

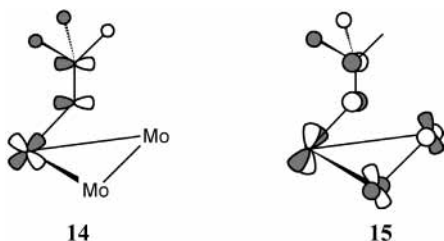
Interestingly, the peaks of the Mo–O bond and C–O COOP coincide. This is a strong indication that the C–O bonding orbitals also carry the most important Mo–O bonding contributions. And, more interestingly, a region of C–O antibonding orbitals below the Fermi level is also Mo–O bonding in character. A detailed examination of the orbitals, discussed below, shows that the wave functions are indeed delocalized over Mo–O–C, so this is not an accidental coincidence of energy levels of different orbitals.

It is surprising, perhaps, to see C–O antibonding character in the chemisorbed cyclopropylmethoxide. This antibonding interaction is not due to adsorption but is already present in the isolated molecule. The effect is also found in the more symmetric molecule methoxide itself. What is happening here is that the π_σ orbital of the methyl group⁵³ forms bonding and antibonding interactions with oxygen lone pairs, resulting in two pairs of degenerate orbitals as shown schematically in **13**. These frontier orbitals of methoxide have been discussed before by our group in connection with adsorption on a nickel surface.⁵⁴

In the unsymmetric cyclopropylmethanol molecule, these MOs are in principle the same, only somewhat distorted, due to σ - π mixing.



In the adsorbate, these C-O bonding and antibonding MOs interact with crystal orbitals of the Mo surface atoms and facilitate adsorbate formation. We show the orbitals here for adsorbed methoxide because they are less distorted by mixing. But we observed the same orbital interaction for cyclopropylmethoxide and believe that this bonding applies to other alkoxide adsorbates as well. Compounds **14** and **15** depict local cutouts of the Mo-O bonding crystal orbitals, corresponding to the two positive Mo-O COOP peaks in Figure 6. The orbital in **14** has Mo-O bonding and C-O bonding character, while **15** shows an orbital that is Mo-O bonding and C-O antibonding. Each of the orbitals shown has a quasidegenerate counterpart, not illustrated here, as implied in **13**. Note in **15** that, in the case of a π -type interaction between O and the Mo atom closest to it, the two other Mo atoms of the quasi-3-fold site can interact with the O atom as well.



Because the C-O bonding and the C-O π -antibonding orbitals are occupied prior to adsorption, the result of the interaction with the metal substrate is the weakening of both. These two effects could, in principle, cancel each other out (no effect on the C-O bond strength). As the calculation shows, a net slight weakening of the C-O bond results; in the case of cyclopropylmethoxide, the C-O bond is elongated in the adsorbate by 9 pm. For methoxide, it is elongated by 4 pm, compared to the respective free alcohols.

The C-C bonds of the cyclopropane ring are not expected to be significantly influenced by the adsorption. In fact, the two almost degenerate HOMOs of the molecule are also the highest

occupied crystal orbitals in the adsorbate (substrate surface states disregarded) shown in **16** and **17**. They are the so-called Walsh orbitals⁵⁵ of cyclopropane, slightly distorted because of the asymmetry in the molecule. Because of this distortion, one of the Walsh orbitals involves not only the distal C-C bond but also the C-C bond that is antiperiplanar to the C-O bond.

Overall, this orbital analysis based on the alcohol molecule and the adsorbed cyclic alkoxide shows that upon thermal excitation of this species the C-C bonds of the three-membered ring will be affected most. Specifically, we expect the greatest effect of a temperature increase for the C-C bond that is antiperiplanar to the C-O bond. The C-O bond is slightly weakened in the adsorbate but not as much to reverse the intrinsic reactivity of the isolated molecule.

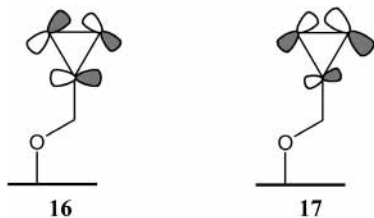
Experimental Implications

The radical clock mechanism is, apparently, not the only mechanism that would lead to the observed transformation. The C-O bond cleavage, the initial step of the radical clock mechanism, requires in our computations on a gas phase isolated molecule a clearly higher energy than the competing C-C bond cleavage of the cyclopropyl ring.

Both mechanisms are consistent with the primary experimental evidence for this transformation, the vanishing ring mode and emerging C=C stretching mode at higher temperatures. Therefore, the reported results about the preference of C-C cleavage in model intermediates do not contradict the experiments. If the species are in close contact with the surface, the C-O bond is expected to be affected somewhat (according to our slab calculations and MO analysis not by much). That's why, on the basis of this analysis, we cannot exclude either mechanism. In the current work, we merely bring up and follow an alternative route for the observed transformation, one that comes to mind from past chemical experience with radical formation and the reactivity of the cyclopropyl ring. We hope to stimulate new theoretical and experimental probes which might eventually determine unambiguously the preferred mechanism and develop further or other radical clocks on surfaces.

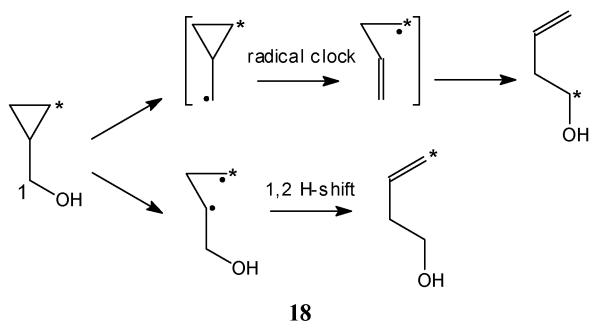
For the isolated molecule, the barrier for the rearrangement of the radical clock following C-O cleavage is so low that overall the radical clock mechanism is still in the same energy range as the competing pathway via a diradical and a 1,2-H shift. This competing pathway has the advantage that it would not involve fragmentation and recombination of the adsorbate. So, the crucial question for the radical clock pathway is whether the cyclopropylmethyl radical stays somehow in the vicinity of the surface so that it is trapped again after its practically instantaneous rearrangement. If it does so, it is possible to have radical clocks for surface reactions. And we have maybe seen in the experiment cited the first radical clock on a surface. To obtain further evidence for this mechanism, we can suggest, on the basis of this theoretical study, some experimental indications.

The stretching frequency of the terminal C=C double bond is about 40 cm^{-1} lower than that for the doubly substituted double bond, as calculated for the isolated butenol molecules and in the cluster models (Table 3). On the radical clock pathway, only the butenol species with a terminal C=C double bond, 3-butenol, can result. In the experiment⁴ that led to the proposed radical clock mechanism, one C=C stretching frequency at 1645 cm^{-1} was found and assigned to adsorbed 3-butenol by comparison with the spectrum of the adsorbate known to be 3-butenol. On the diradical pathway, 2-butenol, with a doubly substituted double bond, would be formed as well. A second, higher-lying frequency, indicating the presence of



2-butenol in the experiment, is not reported. This is a strong indication that only adsorbed 3-butenol is formed and that indeed the radical clock rearrangement occurs. A spectrum of 2-butenol on the surface would be an easy test case; a signal (around 1700 cm^{-1}) can be expected (maybe with low intensity because of the special selection rules of surface-IR spectroscopy) that would not be found in the reported spectrum at 460 K for the reaction product. Studies of the surface chemistry of 2-butenol are currently underway.⁵⁶

Isotope-labeling experiments can bring further clarity to the problem. If one would, for example, label one of the carbon atoms with D or ^{13}C as indicated by the asterisk in **18**, the two pathways would be distinguishable in the reaction product. In the case of the radical clock mechanism, the labeled carbon atom would be the α carbon; in the diradical case, the labeled carbon atom would be the ω carbon. If a carbon isotope labeling would be used, the presence of the ^{13}C in the double bond of the product resulting from the diradical mechanism should lead to an observable shift of $\nu(\text{C}=\text{C})$ to lower frequencies in the infrared spectrum recorded at 460 K.



The synthesis of the cyclopropylmethanol deuterium labeled in the C1 position was successful, and IR experiments with the labeled molecule are currently being carried out.⁵⁷ Preliminary results from this investigation suggest strongly that more than one mechanism for the transformation is at work.

In ^{18}O -labeling experiments already carried out, it was observed that the C–O bond partly incorporates surface oxygen above 460 K, i.e., if the experiment is performed with cyclopropylmethanol on ^{18}O -covered Mo(110).⁴ This strongly suggests cleavage of some of the C–O bonds in the course of the reaction.

Finally, a different radical clock could be used, one that does not involve strong ring strain. The above-mentioned cyclopentylmethyl radical clock would react from the ring-opened hexenyl form to the cyclic form.³ This transformation could be observed by IR spectroscopy in a similar way. Corresponding experiments are being currently carried out. The homologous system with the five-membered ring is somewhat different, as the radical rearranges at a significantly lower rate and the C–O bond strength might vary as well, causing possibly a change of the temperature at which the rearrangement would happen. If it is observed at approximately the same temperature, the radical clock mechanism is at work. The reverse cannot be concluded.

Conclusions

We investigated the possibility of a radical clock mechanism for the observed rearrangement of cyclopropylmethoxy on a surface. There is a possible alternative mechanism that does not involve fragmentation via an initial C–O bond cleavage and recombination of the fragments after the radical clock rearrangement. This mechanism

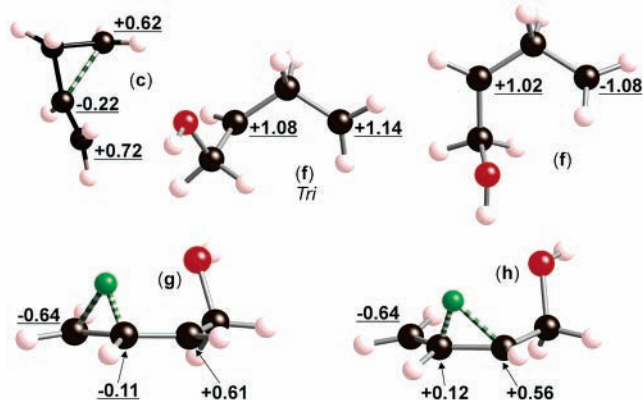


Figure 7. Calculated atomic spin densities for structures of selected open-shell species along the reaction paths: (c) TS of the radical clock rearrangement (doublet); (f) diradical after breakage of vicinal C–C bond in singlet and triplet state (*Tri*); (g) TS of the 1,2-H shift toward the primary carbon radical in the singlet state; (h) TS of the 1,2-H shift toward the secondary carbon radical in the singlet state.

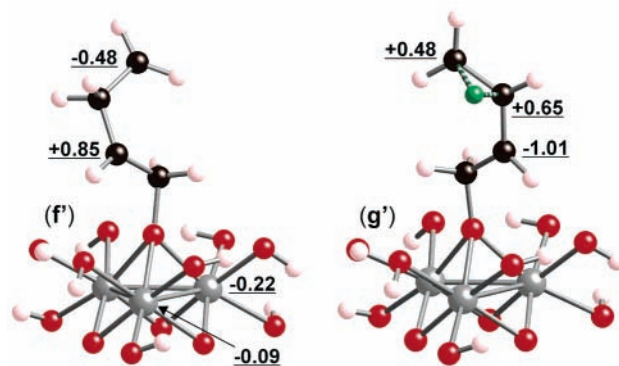


Figure 8. Calculated atomic spin densities for selected open-shell species $[\text{Mo}_3\text{O}_4\text{C}_4\text{H}_7(\text{OH})_6]^+$ along the reaction paths: (f') diradical after breakage of vicinal C–C bond in the singlet state; (g') TS of the 1,2-H shift toward the primary carbon radical in the singlet state.

is indicated by cleavage of the strained three-membered ring and subsequent 1,2-H shift.

Calculated gas-phase relative energies of model systems along the reaction paths show that in the initial step a breakage of the three-membered ring is preferred over a C–O cleavage. This is further supported by an MO analysis. However, the energy barrier for the subsequent 1,2-H shift of the diradical is significantly higher than the barrier for the rearrangement of the cyclopropylmethyl radical. In the gas phase calculations on the isolated molecule, the preference for the singlet diradical pathway is relatively clear. But the two highest points along the pathways become energetically almost indistinguishable if one looks at the cluster model calculations. Therefore, the radical clock mechanism is overall in a reasonable energy region, and the competing pathway is in our molecular model calculations only insignificantly preferred.

We think it is likely that on the surface both mechanisms are at work. To get a more definite answer on the preferred mechanism from calculations, one would have to be able to calculate a diradical on an extended surface slab model in a defined singlet spin state. This pushes the limit of currently available theoretical methods. Several further experimental probes of the reaction mechanism are suggested.

Acknowledgment. We are grateful to the National Science Foundation for the support of this research by a Grant, CHE 02-04841. The DFG is acknowledged for providing an Emmy-

Noether fellowship for B.F. We thank Dean Tantillo for helpful and interesting discussions. I.K. thanks the Alexander von Humboldt foundation for a Feodor-Lynen fellowship.

Appendix

In Figures 7 and 8, we show significant atomic spin densities that were calculated for open-shell doublet, singlet, and triplet systems.

References and Notes

- Bowry, V. W.; Ingold, K. U. *J. Am. Chem. Soc.* **1991**, *113*, 5699–5707.
- Engel, P. S.; Keys, D. E.; Kitamura, A. *J. Am. Chem. Soc.* **1985**, *107*, 4964–4975.
- Griller, D.; Ingold, K. U. *Acc. Chem. Res.* **1980**, *13*, 317–323.
- Kretzschmar, I.; Levinson, J. A.; Friend, C. M. *J. Am. Chem. Soc.* **2000**, *122*, 12395–12396.
- Kretzschmar, I.; Friend, C. M. *J. Phys. Chem. B* **2002**, *106*(33), 8407–8414.
- Lunsford, J. H. *Angew. Chem., Int. Ed. Engl.* **1995**, *34*, 970–980.
- Horn, A. H. C.; Clark, T. *J. Am. Chem. Soc.* **2003**, *125*, 2809–2816.
- Cooksy, A. L.; King, H. F.; Richardson, W. H. *J. Org. Chem.* **2003**, *68*, 9441–9452.
- Levinson, J. A.; Kretzschmar, I.; Sheehy, M. A.; Deiner, L. J.; Friend, C. M. *Surf. Sci.* **2001**, *479*, 273–286.
- Bockstedte, M.; Kley, A.; Neugebauer, J.; Scheffler, M. *Comput. Phys. Comm.* **1997**, *107*, 187–222.
- Troullier, N.; Martins, J. L. *Phys. Rev.* **1991**, *B 43*, 1993–2006.
- Fuchs, M.; Scheffler, M. *Comput. Phys. Comm.* **1999**, *119*, 67–98.
- Gonze, X.; Stumpf, R.; Scheffler, M. *Phys. Rev. B* **1991**, *44*, 8503–8513.
- Monkhorst, H. J.; Pack, J. D. *Phys. Rev.* **1976**, *B13*, 5188–5192.
- Perdew, J.; Zunger, A. *Phys. Rev.* **1981**, *B 23*, 5048–5079.
- (a) Becke, A. D. *Phys. Rev.* **1988**, *A 38*, 3098–3100. (b) Perdew, J. P. *Phys. Rev.* **1986**, *B33*, 8822–8824.
- Donohue, J. *The Structures of the Elements*; Krieger, R. E., Ed.; Malabar, Florida; 186.
- Morales de la Garza, L.; Clarke, L. J. *J. Phys. C: Solid State Phys.* **1981**, *14*, 5391–5401.
- Becke, A. D. *J. Chem. Phys.* **1993**, *98*, 5648–5652.
- Frisch, M. J.; Trucks, G. W.; Schlegel, H. B.; Scuseria, G. E.; Robb, M. A.; Cheeseman, J. R.; Zakrzewski, V. G.; Montgomery, J. A., Jr.; Stratmann, R. E.; Burant, J. C.; Dapprich, S.; Millam, J. M.; Daniels, A. D.; Kudin, K. N.; Strain, M. C.; Farkas, O.; Tomasi, J.; Barone, V.; Cossi, M.; Cammi, R.; Mennucci, B.; Pomelli, C.; Adamo, C.; Clifford, S.; Ochterski, J.; Petersson, G. A.; Ayala, P. Y.; Cui, Q.; Morokuma, K.; Malick, D. K.; Rabuck, A. D.; Raghavachari, K.; Foresman, J. B.; Cioslowski, J.; Ortiz, J. V.; Stefanov, B. B.; Liu, G.; Liashenko, A.; Piskorz, P.; Komaromi, I.; Gomperts, R.; Martin, R. L.; Fox, D. J.; Keith, T.; Al-Laham, M. A.; Peng, C. Y.; Nanayakkara, A.; Gonzalez, C.; Challacombe, M.; Gill, P. M. W.; Johnson, B. G.; Chen, W.; Wong, M. W.; Andres, J. L.; Head-Gordon, M.; Replogle, E. S.; Pople, J. A. *Gaussian 98*, revision A.9; Gaussian, Inc.: Pittsburgh, PA, 1998.
- Modern Theoretical Chemistry*; Schaefer, H. F., III, Ed.; Plenum: New York, 1976; pp 1–28.
- Hay, P. J.; Wadt, W. R. *J. Chem. Phys.* **1985**, *82*, 299–310.
- Landrum, G. A.; Glassey, W. V. <http://sourceforge.net/projects/yachmop/>, 1999.
- Jean, Y.; Lledos, A.; Burdett, J. K.; Hoffmann, R. *J. Am. Chem. Soc.* **1988**, *110*, 4506–4516.
- Hoffmann, R. *J. Chem. Phys.* **1963**, *39*, 1397–1412.
- Mealli, C.; Proserpio, D. M. *J. Chem. Educ.* **1990**, *67*, 399–402.
- Colaianni, M. L.; Chen, J. G.; Weinberg, W. H.; Yates, J. T. *Surf. Sci.* **1992**, *279*, 211–222.
- Flemmig, B.; Hoffmann, R. Unpublished results: calculations of the oxygen overlayer on Mo (110) with $\theta = 1/2$ in different variations and $\theta = 2/3$.
- Flemmig, B.; Szargan, R.; Reinhold, J. *J. Phys. Chem. B* **2001**, *105*, 5440–5449.
- Wilcox, C. F.; Loew, L. M.; Hoffmann, R. *J. Am. Chem. Soc.* **1973**, *95*, 8192–8193.
- Calculations with HOMO–LUMO mixing in the initial guess did lead to an open-shell singlet wave function (α and β spin electron in different orbitals) if an appropriate ring-opened start geometry was used.
- Hoffmann, R. *J. Am. Chem. Soc.* **1968**, *90*, 1475–1485.
- Fan, K.-N.; Li, Z.-H.; Wang, W.-N.; Huang, H.-H.; Huang, W. *Chem. Phys. Lett.* **1997**, *277*, 257–263.
- Dubnikova, F.; Lifshitz, A. *J. Phys. Chem. A* **1998**, *102*, 3299–3306.
- Bettinger, H. F.; Rienstra-Kiracofe, J. C.; Hoffman, B. C.; Schaefer, H. F., III; Baldwin, J. E.; Schleyer, P. v. R. *Chem. Commun.* **1999**, 1515–1516.
- Pedersen, S.; Herek, J. L.; Zewail, A. H. *Science* **1994**, *266*, 1359–1364.
- Baldwin, J. E.; Burrell, R. C.; Shukla, R. *Org. Lett.* **2002**, *4*, 3305–3307.
- Hassenrück, K.; Martin, H.-D.; Walsh, R. *Chem. Ber.* **1988**, *121*, 369–372.
- Bart, S. C.; Chirik, P. J. *J. Am. Chem. Soc.* **2003**, *125*, 886–887.
- Martel, R.; McBreen, P. H. *J. Chem. Phys.* **1997**, *20*, 8619–8626.
- Glasstone, S.; Laidler, K. J.; Eyring, H. *The Theory of Rate Processes*; McGraw-Hill: New York, 1941; p 100.
- Bergman, R. G. *Diradicals*. In *Free Radicals*; Kochi, J. K., Ed.; Wiley: New York, 1973; pp 191–237.
- Smith, D. M.; Nicolaidis, A.; Golding, B. T.; Radom, L. *J. Am. Chem. Soc.* **1998**, *120*, 10223–10233.
- Maillard, B.; Forrest, D.; Ingold, K. U. *J. Am. Chem. Soc.* **1976**, *98*, 7024–7026.
- Martinez, F. N.; Schlegel, H. B.; Newcomb, M. *J. Org. Chem.* **1996**, *61*, 8547–8550.
- Christen, H. R.; Vögtle, F. *Organische Chemie Band I*; Verlag Salle und Sauerländer: Frankfurt, 1988; p 100.
- Nevill, S. M.; Pincock, A. L.; Pincock, J. A. *J. Org. Chem.* **1997**, *62*, 2680–2681.
- Saeyes, M.; Reyniers, M. F.; Marin, G. B.; Neurock, M. *J. Phys. Chem.* **2002**, *B 106*, 7489–7498.
- Jing, Z.; Whitten, J. L. *Surf. Sci.* **1991**, *250*, 147–158.
- Holleman, A. F.; Wiberg, N. *Lehrbuch der Anorganischen Chemie*; de Gruyter: Berlin, 1985; p 1100.
- Bino, A.; Cotton, F. A.; Dori, Z. *J. Am. Chem. Soc.* **1978**, *100*, 5252–5253.
- Jiang, Y.; Tang, A.; Hoffmann, R.; Huang, J.; Lu, J. *Organometallics* **1985**, *4*, 27–34.
- Jorgensen, W. L.; Salem, L. *The Organic Chemist's Book of Orbitals*; Academic Press: New York, 1973; p 66.
- Zeroka, D.; Hoffmann, R. *Langmuir* **1986**, *2*, 553–558.
- Walsh, A. D. *Trans. Faraday Soc.* **1949**, *45*, 179–190.
- Preliminary results that were obtained during the revision of this paper indicate that the infrared spectrum for 2-butenol on the surface is not the same as for the product of the hydroxymethylcyclopropane.
- Kang, D. H.; Friend, C. M.; Wiedemann, S.; Bergman, R. G. Private communication.